catalysts

MDPI

Review

Heterogeneous Metal-Activated Persulfate and Electrochemically Activated Persulfate: A Review

Junjing Li [1,*], Yiqi Liang [1], Pengliang Jin [1], Bin Zhao [1], Zhaohui Zhang [1], Xiaojia He [2], Zilin Tan [1], Liang Wang [1,*] and Xiuwen Cheng [3,*]

1 School of Environmental Science and Engineering, Tiangong University, State Key Laboratory of Separation Membranes and Membrane Processes, Tianjin Municipal Key Lab of Advanced Fiber and Energy Storage Technology, Binshui West Road 399, Xiqing District, Tianjin 300387, China
2 The Administrative Center for China's Agenda 21, Beijing 100038, China
3 Key Laboratory for Environmental Pollution Prediction and Control, Gansu Province, College of Earth and Environmental Sciences, Lanzhou University, Lanzhou 730000, China
* Correspondence: junjingli85@163.com (J.L.); mashi7822@163.com (L.W.); chengxw@lzu.edu.cn (X.C.)

Abstract: The problem of organic pollution in wastewater is an important challenge due to its negative impact on the aquatic environment and human health. This review provides an outline of the research status for a sulfate-based advanced oxidation process in the removal of organic pollutants from water. The progress for metal catalyst activation and electrochemical activation is summarized including the use of catalyst-activated peroxymonosulfate (PMS) and peroxydisulfate (PDS) to generate hydroxyl radicals and sulfate radicals to degrade pollutants in water. This review covers mainly single metal (e.g., cobalt, copper, iron and manganese) and mixed metal catalyst activation as well as electrochemical activation in recent years. The leaching of metal ions in transition metal catalysts, the application of mixed metals, and the combination with the electrochemical process are summarized. The research and development process of the electrochemical activation process for the degradation of the main pollutants is also described in detail.

Keywords: sulfate-based advanced oxidation process; metal catalyst activation; electrochemical activation; sulfate radicals; wastewater

Citation: Li, J.; Liang, Y.; Jin, P.; Zhao, B.; Zhang, Z.; He, X.; Tan, Z.; Wang, L.; Cheng, X. Heterogeneous Metal-Activated Persulfate and Electrochemically Activated Persulfate: A Review. *Catalysts* **2022**, *12*, 1024. https://doi.org/10.3390/catal12091024

Academic Editors: Jiangkun Du, Lie Yang and Chengdu Qi

Received: 20 August 2022
Accepted: 6 September 2022
Published: 9 September 2022

1. Introduction

In recent decades, the organic pollutants that cause water pollution have increased. Many refractory organic compounds in wastewater are toxic, and it is very difficult to remove them by using conventional treatment methods; therefore, the removal of refractory organic pollutants has become a challenging problem. The water pollution caused by some emerging organic pollutants might seriously affect the ecological balance and further threaten human health [1–3]; therefore, it is meaningful to study more efficient water treatment technologies. Sulfate radical advanced oxidation is an effective process for the treatment of organic pollutants in wastewater. In this process, the degradation of pollutants depends mainly on the free radicals produced and sulfate radicals and hydroxyl radicals are the main reactive oxygen species, which play a key role in the degradation of pollutants [4–6]. Sulfate radicals and hydroxyl radicals have a good treatment effect on endocrine disruptors [7], drugs and metabolites [8,9], cyanide toxins [10,11], perfluorinated compounds [12], and other refractory pollutants in wastewater. The activation of persulfate by transition metals in heterogeneous systems is more cost-effective than thermal [13], ultraviolet [14,15], and ultrasonic activation methods [16]. Moreover, in heterogeneous systems for persulfate activation, it is easier to separate a catalyst from the wastewater and it has been shown to exhibit a greater tolerance to extreme operating conditions [17–19]. Additionally, cobalt, copper, iron and manganese-based catalysts are usually used in heterogeneous systems [20–22]; therefore, a review on heterogeneous systems for persulfate

activation is needed. The electrochemical activation of the persulfate process, a new process with potential applications, has the advantages of high efficiency, easy operation, strong processing capacity, and an avoidance of secondary pollution [23,24]. The role of anodic and cathodic processes in the electrochemical activation of persulfate was studied. The formation of sulfate radicals on boron doped diamond (BDD) anodes and the activation of persulfate on graphite cathodes have been elucidated using different electrolytes and electrochemical devices [25]. For example, the electrochemical activation of the persulfate for atrazine (ATZ) degradation was studied using novel B, a co-doped TiO_2 anode. Stainless steel, carbon felt and a carbon black-modified carbon felt were used for the cathode, respectively. The main reactive oxygen species in the different systems were different [26].

In this paper, the research progress of metal-based heterogeneous catalysts and electrochemical activation processes to remove organic pollutants in wastewater is reviewed. The research progress of persulfate activation is mainly introduced. Persulfate activation is related mainly to the single metal catalyst, mixed metal catalyst, and electrochemical processes. In addition, the study of carbon anodes and carbon cathodes in electrochemical activation processes is also included.

2. The Activation of Persulfates

The properties of persulfates (PS), activation methods and the effect of the reaction conditions on the activation process of persulfate are summarized.

2.1. The Properties of Persulfates

In the advanced oxidation process (AOP), oxidized free radicals with high activity are produced, such as sulfate radicals ($SO_4^{\bullet -}$, E_0 = 2.5–3.1 eV) and hydroxyl radicals ($^{\bullet}HO$, E_0 = 1.89–2.72 eV). Peroxomonosulfate (PMS) has an unsymmetrical structure because only one H is replaced by SO_3. The electron cloud of the O-O bond is inclined to the SO_3 side, making the O of the H-side carry positive charges because SO_3 can attract electrons. These peroxides are good oxidizers with a standard oxidation-reduction potential (E_0) of 2.01 eV (peroxydisulfate, PDS) [27] and 1.82 eV (PMS) [28–30].

The activation of persulfates (including PMS and PDS) is a common method to produce $SO_4^{\bullet -}$. Sulfate radical ($SO_4^{\bullet -}$) oxidation is an effective method for removing organic pollutants from water [31–33]. Additionally, $SO_4^{\bullet -}$ has an ultrahigh redox potential. Compared with PDS, the advantage of PMS lies in its asymmetric structure [34]. Because of its slow reaction with organic compounds, persulfate (Equation (1)) has relatively stable chemical properties [31]; after activation (Equations (2)–(5)), persulfate can produce $SO_4^{\bullet -}$ (oxidation potential: 2.4 eV) and $^{\bullet}OH$ (oxidation potential: 2.8 eV) to degrade pollutants [31,35,36]:

$$S_2O_8^{2-} + 2e^- \rightarrow 2SO_4^{2-} \quad (1)$$

$$S_2O_8^{2-} \overset{heat}{\rightarrow} 2SO_4^{\bullet -} \quad (2)$$

$$2S_2O_8^{2-} + 2H_2O \overset{OH^-}{\rightarrow} SO_4^{\bullet -} + 3SO_4^{2-} + O_2^{\bullet -} + 4H^+ \quad (3)$$

$$S_2O_8^{2-} + Fe^{2+} \overset{OH^-}{\rightarrow} SO_4^{\bullet -} + SO_4^{2-} + Fe^{3+} \quad (4)$$

$$SO_4^{\bullet -} + H_2O \rightarrow {}^{\bullet}OH + SO_4^{2-} + H^+ \quad (5)$$

2.2. Activation Methods

The persulfate activation methods include ultraviolet rays, ultrasound, thermal, transition metals, carbon-based catalysts, etc. These aspects are introduced in the following sections.

Ultraviolet rays are the most economical among several activation methods (e.g., UV, gamma-ray, etc.) (6):

$$S_2O_4^{2-} + hv \rightarrow 2SO_4^{\bullet -} \quad (6)$$

Ultrasound has the advantages of safety and having no secondary pollution, but a narrow range of action is its limitation [37]. The removal of atrazine by thermally activated persulfate follows a pseudo-first-order reaction model [13]. Compared with the single condition, the effect of thermal and ultraviolet light on the degradation of organic pollutants in concentrated leachate is better [38], but for all of that, there is an external energy cost. Transition metals activate persulfate in a uniform form and produce free radicals by the same mechanism (7):

$$M^{2+} + PS \rightarrow M^{(n+1)+} + \text{sulfate radical} + \text{sulfate ion} \quad (7)$$

where M represents the metal [29].

In inhomogeneous materials, carbon-based catalysts provide potential activation methods. The mechanism of free radical formation by the activation of organic compounds is shown in Equation (8) [39]:

$$\text{organic} + PS \rightarrow \text{intermediates} + \text{sulfate radical} + \text{sulfate ion} \quad (8)$$

2.3. The Effect of Reaction Conditions

The generation of free radicals, the solution pH, reactant concentration, and the interaction of coexisting ions have a great influence on the degradation of pollutants. The activation of persulfate is very different under different pH conditions and different activation factors require different pH values. For example, transition metals require an acidic environment for activation, but metal-doped carbon-based catalysts are not suitable for low pH [40]. Carbonate and chloride might play an important role in activated persulfate [41]. Natural organic compounds can be used as the free radical scavengers of active species, which can reduce the removal efficiency of organic pollutants. Under a neutral pH, the activation of persulfate by iron is not affected by too many substances.

3. Heterogeneous Transition Metal Catalysts

The species of mainly studied heterogeneous transition metal catalysts were shown in Figure 1.

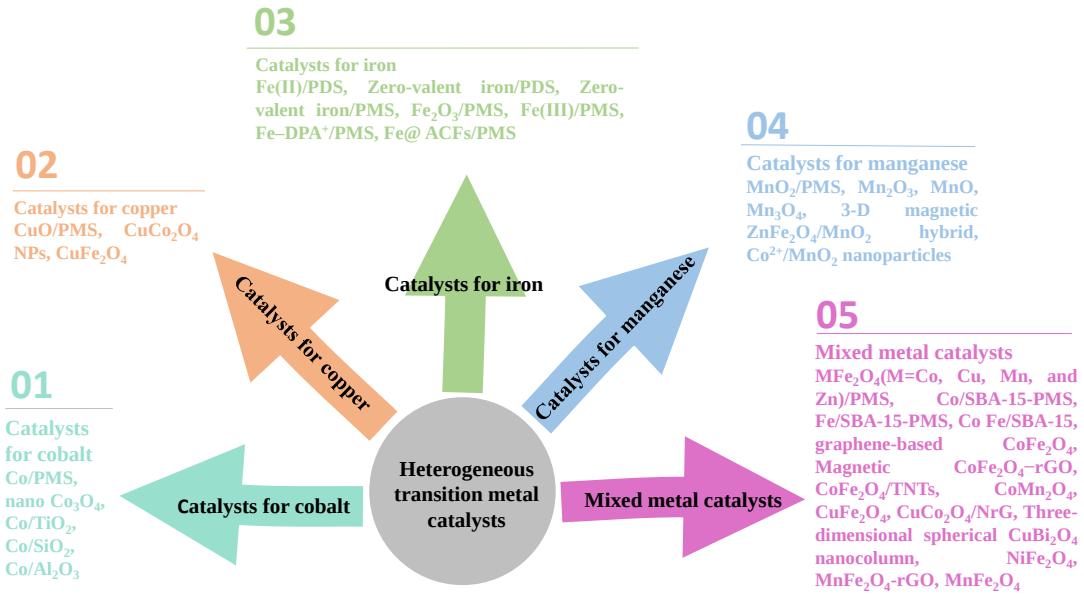

Figure 1. The species of heterogeneous transition metal catalysts.

3.1. Catalysts for Cobalt

The Co/PMS system has a high efficiency over a wide pH range and a high efficiency in bicarbonate and carbonate buffers; however, the toxicity of cobalt leads to additional

costs for precipitation and separation after activation. To reduce leaching, for example, nanoCo_3O_4 has previously been prepared. The system had good heterogeneous activity and a low leaching rate under neutral conditions [42]. In some studies, the degradation effect of 2,4-dichlorophenol was good in heterogeneous systems under neutral conditions, and the concentration of cobalt ions dissolved from Co_3O_4 was 70 $\mu g \cdot L^{-1}$ [43]. Among $Co/TiO_2{}^-$, Co/SiO_2- and Co/Al_2O_3-supported cobalt oxides, the catalytic degradation effect of phenol on Co/TiO_2 was the best and had a more stable performance. The factors affecting the catalyst activity were related mainly to the leaching of Co, intermediate products, and a change in the surface charge [44].

3.2. Catalysts for Copper

Copper has the advantages of being nontoxic and inexpensive and is suitable for preparing catalysts. Heterogeneous CuO can activate PMS to generate sulfate radicals. When copper is loaded on Zeolite Socony Mobile-Five (ZSM5), the large surface area of the ZSM5 enhances the catalytic reaction. The synergy between the two makes the catalytic efficiency higher than the catalytic efficiency of pure CuO [45]. The degradation efficiency in the CuO/H_2O_2 Fenton-like system is significantly lower than the degradation efficiency in the CuO/Oxone system. Moreover, the catalytic activity of $CuCo_2O_4$ nanoparticles prepared by the solvothermal method for PMS activation is the highest among the activators ($CuCo_2O_4$, $CuFe_2O_4$, Co_3O_4, CuO, and Fe_3O_4). Of course, $CuCo_2O_4$ nanoparticles are highly stable during catalytic reactions and have a very good reusability [46]. Under the influence of Cu^{2+}/PS, the main active substances for the degradation of sulfamethazine (SMZ) are sulfate radicals and hydroxyl radicals. In the process of the reaction, the complex formed by Cu^{2+} and SMZ also affects SMZ degradation [47]. CuO catalysts prepared by the hydrothermal method can effectively activate PS to degrade methylene blue (MB). After five continuous catalytic batches, its degradation can still reach approximately 70% [48].

3.3. Catalysts for Iron

The Fe^{2+}-activated PDS system can be applied to wastewater treatment; however, under acidic conditions, excess Fe^{2+} reacts with sulfate radicals generated by activation, resulting in a decrease in the degradation efficiency (Equations (9) and (10)).

$$S_2O_8^{2-} + Fe^{2+} \rightarrow SO_4^{\bullet -} + SO_4^{2-} + Fe^{3+} \quad (9)$$

$$SO_4^{\bullet -} + Fe^{2+} \rightarrow SO_4^{2-} + Fe^{3+} \quad (10)$$

The zero-valent iron (ZVI)/PDS activation system, for example, significantly increased the removal of 4-chlorophenol [49]. Furthermore, the ZVI/PDS activation system has been shown to have a good performance on naphthalene, trichloroethylene, anthraquinone dye, polyvinyl alcohol, and 2,4-dinitrotoluene removal [49–53]. Additionally, the ZVI/PMS system can completely remove both Brij 35 and Cr^{4+} from an aqueous solution [54]. In the ZVI/PMS system for the degradation of *p*-chloraniline (PCA), ZVI is the activator of ferrous ions for generating sulfate radicals [55] and compared with zero-valent copper, ZVI has a higher efficiency in decolorization and has the advantages of environmental protection, economy and nontoxicity [56]. The molar ratio of persulfate to Fe^{2+} or Fe^0 is 1:1, and polyvinyl alcohol (PVA) can be completely oxidized in the persulfate and ZVI system; however, PVA cannot be completely oxidized in the Fe^{2+} system [52].

The porous Fe_2O_3/PMS system has shown good results in the treatment of rhodamine B [57]. For the degradation of polychlorinated biphenyls, the free radical pathway plays an important role in the Fe^{2+}/PMS system. In the Fe^{3+}/PMS system, there are sulfate radicals and hydroxyl radicals [56]. In the removal of bisphenol A (BPA), the homogeneous Fe-dipicolinic acid/PMS system has a better effect than the Fe^{3+}/PMS system. In addition, compared with Co_3O_4 with its cobalt leaching problems, dipicolinic acid-functionalized hematite has more environmentally friendly and economical advantages while ensuring the removal efficiency and rate [58]. The Fe@ACF/PMS system shows a higher oxygen uti-

lization rate and lower activation energy than the Fe@ACF/H_2O_2 system. Fe@ACFs/PMS is a promising and efficient green processing technology [59]. In the Fe_3O_4 magnetic nanoparticle (MNP)/PMS system, hydroxyl radicals and sulfate radicals are the main active species in the degradation of acetaminophen [60]. For example, iron ions were restricted due to the formation of hydroxides, and activated carbon fibers (ACFs) were introduced as a support material. ACFs have a large surface area and high adsorption capacity and here, ACFs supported ferric oxalate (FeOxa) to form a new type of catalyst, FeOxa@ACFs. The FeOxa@ACFs were capable of excellent recyclability and had a broad pH adaptability (3.0–10.0) [61]. Elsewhere, the degradation of amoxicillin by iron persulfate activated on activated carbon had good catalytic activity and an obvious detoxification of amoxicillin (AMO) under mild conditions [62]. A biochar-supported nanosized iron (nFe^0/BC) was constructed and it was an effective activator for PS for the degradation of tetracycline. Sulfate radicals and hydroxyl radicals played critical roles in the degradation of tetracycline. Additionally, nFe^0/BC is relatively stable and is a promising PS activator [63]. A Fe_3O_4-impregnated graphene oxide (Fe_3O_4@GO) nanocomposite was prepared and was employed as a good persulfate activator for the removal of dye pollutants in real wastewater [64]. The vanadium titanium magnetite (VTM)/PDS system was used to remove methyl orange (MO) decolorization. The reaction system was stable in a wide range of pH values from 3 to 11 and a relatively wide range of MO concentrations from 30 mg·L^{-1} to 120 mg·L^{-1}. The MO was removed by adsorption on the VTM surface and oxidation by $SO_4^{\bullet -}$, produced by the activation of persulfate with Fe^{2+} provided by the VTM [65]. Pyrite could effectively activate PS for the removal of Orange G (OG) in an aqueous solution, where a lower solution pH, higher pyrite dosage and smaller pyrite particles were beneficial for the OG removal [66]. Moreover, the Fe(II)-PS- hydrothermal treatment of sewage sludge could significantly improve the removal efficiency of N at 150 °C when compared with a hydrothermal treatment [67].

3.4. Catalysts for Manganese

There is a wide range of applications for the stable oxides formed by manganese. Oxides with different valence states also have different effects on activating persulfate to degrade pollutants. The order of the catalytic activity of manganese oxides is as follows: Mn_2O_3 > MnO > Mn_3O_4 > MnO_2. This ordering shows that the catalytic activity is related to the oxidation state of manganese. Compared with Mn^{2+} and most heterogeneous cobalt systems, Mn_2O_3 is more effective in the degradation of phenol [68]. The catalytic sequence of α-Mn_2O_3 activating PMS is α-Mn_2O_3-cubic > α-Mn_2O_3-octahedra > α-Mn_2O_3-truncated; however, the efficient degradation of phenol depends on a high specific surface area, phenol adsorption, and surface activity [69]. The reaction process of PMS activated by manganese dioxide [70] can be summarized as follows:

$$HSO_5^- + 2MnO_2 \rightarrow SO_5^{2-} + OH^- + Mn_2O_3 \quad (11)$$

$$HSO_5^- + Mn_2O_3 \rightarrow SO_4^{\bullet -} + H^+ + 2MnO_2 \quad (12)$$

$$SO_4^{\bullet -} + H_2O \rightarrow {}^{\bullet}HO + H^+ + SO_4^{2-} \quad (13)$$

$$C_6H_5OH + SO_4^{\bullet -} \rightarrow \text{several steps} \rightarrow CO_2 + H_2O + SO_4^{2-} \quad (14)$$

In the study of one-dimensional α-MnO_2 nanostructures and sulfate radicals, among Mn nanowires, Mn nanorods, and Mn nanotubes, the Mn nanowires have the best performance for the degradation of phenol. The main reactive oxygen species (ROS) is sulfate radicals (Figure 2) [19,71].

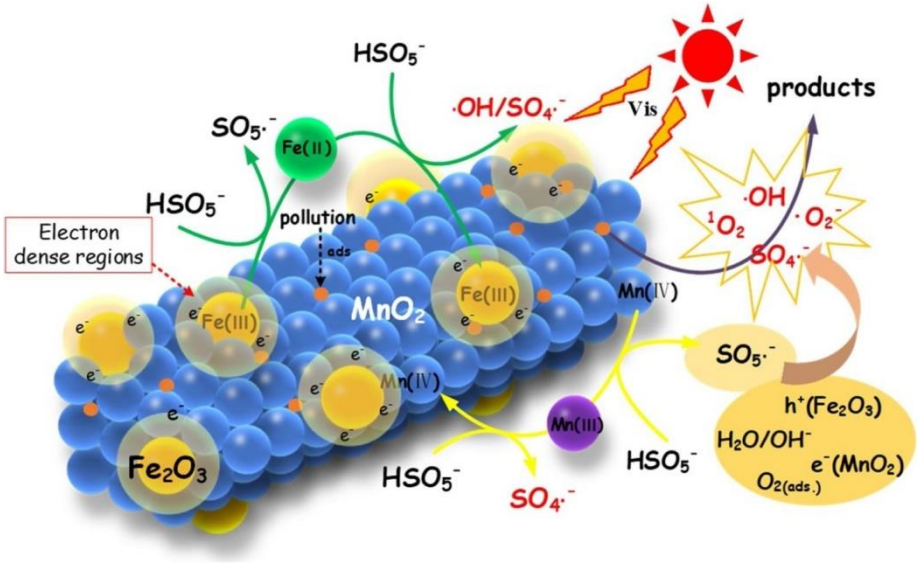

Figure 2. The reaction mechanism for the removal of organic pollutants in the nanohybrid MnO_2 incorporating a Fe_2O_3/PMS/Vis system. Reprinted with permission from ref. [19]. Copyright 2020 Elsevier B.V.

The cost of magnetic separation is lower than the cost of the traditional separation process. The catalyst can be easily extracted from an aqueous solution by the action of an external magnetic field. The magnetic manganese catalyst prepared by using Fe_3O_4 as the magnetic core, carbon spheres as a barrier, and Mn as the functional component has a better catalytic performance than commercial MnO_2 and Fe_3O_4, while Mn species on magnetic carbon nanospheres (MCSs) can provide a higher phenol removal efficiency [72]. For example, the 3D magnetic $ZnFe_2O_4/MnO_2$ hybrid catalysts were synthesized by a hydrothermal method and the results showed that $ZnFe_2O_4/MnO_2$ had a better catalytic performance than sea urchin catalysts due to its high specific surface area [73]. The manganese oxide catalysts were synthesized by a simple coprecipitation method. The Mn_3O_4 nanoparticles with a tetragonal structure showed a good catalytic performance for the degradation of red G (ARG) by activating PMS to produce free radicals. By precipitation, the catalyst can be separated and can maintain good catalytic activity. The synthesized catalyst has a good stability and reusability [74]. Additionally, the combination of activated PMS, Co_3O_4, and MnO_2 had a synergistic effect on the degradation of phenol. At low temperatures, Co^{2+}/MnO_2 nanoparticles had a stronger redox ability, stable performance during recycling, and a better activation performance than Co/MnO_2 [75]. Elsewhere, Fe_3O_4/MnO_2 core-shell composites with a low cost and little hazard were prepared by a one-pot method. The activation of PMS was carried out on the surface of the material, and not by metal ions in the solution. When the molar ratio of Fe/Mn was 4:1, the catalytic effect of magnetic Fe_3O_4/MnO_2 nanocomposites on the degradation of 4-chlorophenol (4-CP) by PMS was better than the catalytic effect of other mole ratios [76].

There are mixed manganese species, Mn^{4+} and Mn^{3+}, on the surface of the octahedral molecular sieve (OMS-2) catalyst, which causes the OMS-2 catalyst to have good catalytic activity. When the pH was 7.32, the catalyst was stable over five cycles, and the removal efficiency of Acid Orange 7 (AO7) was more than 90%. The mechanism by which the OMS-2 catalyst activates PMS [77] can be summarized as follows:

$$Mn^{4+} + HSO_5^- \rightarrow Mn^{3+} + SO_5^{\bullet -} + H^+ \quad (15)$$

$$Mn^{3+} + HSO_5^- \rightarrow Mn^{4+} + SO_4^{\bullet -} + OH^- \quad (16)$$

$$SO_4^{\bullet -} + H_2O \rightarrow {}^{\bullet}HO + SO_4^{2-} + H^+ \quad (17)$$

3.5. Mixed Metal Catalysts

To give metal catalysts better stability, scholars are no longer limited to single metal catalysts. A variety of mixed metal catalysts are also used in this catalytic process. Magnetic iron spinel MFe_2O_4 (Co, Cu, Mn, and Zn) was prepared by the sol-gel method to degrade di-*n*-butyl phthalate (DBP) by activating PMS. The sequence of the reducibility of the catalyst in a PMS solution is $CoFe_2O_4$ > $CuFe_2O_4$ > $MnFe_2O_4$ > $ZnFe_2O_4$. In addition, the degradation effect of the PMS solution on DBP was the best under the coaction of Co and Fe. $CoFe_2O_4$, $CuFe_2O_4$, and $MnFe_2O_4$ all had good magnetic properties and were easy to separate and recover in magnetic fields [78]. The mixed spinel oxide of Fe/Co supported on nanoCo_3O_4 and MgO was a very effective heterogeneous catalyst for the oxidative degradation of AO7 in an aqueous solution with PMS as the oxidant. While nanoCo_3O_4 has a better removal performance, MgO is more environmentally friendly, while considering costs, the MgO is cheaper to manufacture, which is also an advantage [79].

A cobalt-iron bimetallic catalyst has a good application in activating a persulfate system (Figure 3) [80]. The Co/SBA-15-PMS system has high catalytic activity, but it is not easy to recover whereas the Fe/SBA-15-PMS system is the opposite. The presence of cobalt in CoFe/SBA-15 gives an excellent catalytic performance, while the presence of iron, which has different active sites and magnetic properties, makes the catalyst easy to separate. The CoFe/SBA-15 has a good effect in the removal of rhodamine B [81]. To improve the performance of $CoFe_2O_4$, for example, researchers introduced graphene into the system. Graphene-based $CoFe_2O_4$ is more effective than $CoFe_2O_4$ in activating PMS for dimethyl phthalate degradation. The effect of graphene is similar to the effect of substrates used to adsorb dimethyl phthalate (DMP) molecules. The optimal proportion of graphene is 22%, with higher concentrations leading to an over-resolution and incomplete DMP degradation. Graphene acts as a matrix rather than a catalyst in the composite catalyst and can adsorb DMP molecules [82]. $CoFe_2O_4$ nanoparticles at a size of 23.8 nm were loaded onto graphene sheets, and $CoFe_2O_4$-rGO hybrids showed a better catalytic performance than pure $CoFe_2O_4$ [83]. Multilayer titanate nanotubes (TNTs) have excellent ion exchange ability due to their unique structural characteristics. Under mild conditions, they can remove various toxic cations and locate free cations through electrostatic interactions and here, TNTs were used as catalyst carriers. The $CoFe_2O_4$/TNTs were prepared by dipping and roasting. Nanosized $CoFe_2O_4$ particles have a small particle size, good dispersion, and a large surface area of hybrid products. The ion exchangeability of the TNT carriers reduced the leaching rate of cobalt [84]. The $CoMn_2O_4$ catalyst is an effective and environmentally friendly catalyst for activating PMS and the high catalytic performance has been attributed to the synergistic effect of Co^{2+}/Co^{3+}, Mn^{2+}/Mn^{3+}, and Mn^{3+}/Mn^{4+} redox pairs [85].

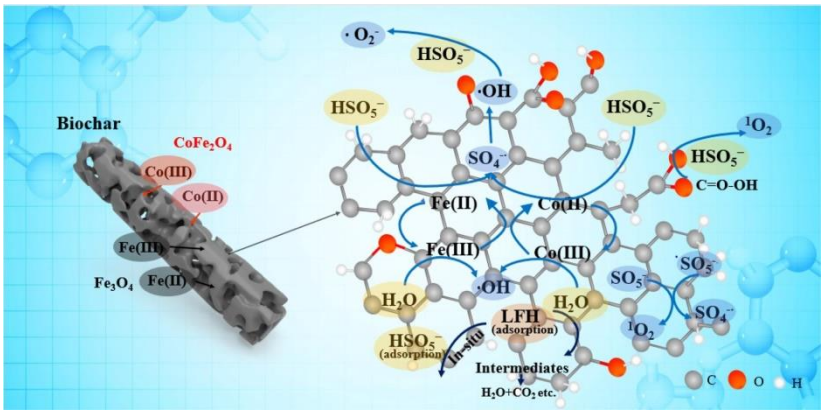

Figure 3. Possible mechanism of magnetic biochar/$CoFe_2O_4$/PMS system for lomefloxacin hydrochloride degradation. Reprinted with permission from ref. [80]. Copyright 2021 Elsevier B.V.

$CuFe_2O_4$ magnetic nanoparticles were used as catalysts to activate PMS. The degradation of tetrabromobisphenol A in the presence of PMS showed a higher catalytic activity

for $CuFe_2O_4$ magnetic nanoparticles compared with Fe_2O_3 and CuO [86]. The magnetic activated carbon composite (MACC) is magnetic and can be easily separated from a solution. A magnetic activated carbon composite ($CuFe_2O_4$/AC) was prepared by a two-step coprecipitation and calcination [87]. In a study of the degradation of bisphenol A by $CuFe_2O_4$MNP-activated PMS, the synergistic effect of the redox pair of Cu^+/Cu^{2+} and Fe^{2+}/Fe^{3+} improved its catalytic activity [88].

A new, efficient, $CuCo_2O_4$/nitrogenated graphene (NrGO) electrocatalyst for pollutant removal has been developed. The results have shown that the nitrogen-doped graphene network enhanced the electron transport and promoted the high oxygen evolution activity of the $CuCo_2O_4$ nanoparticle/NrGO flake composites. The stability of the catalyst was excellent, which was better than the stability of iridium dioxide and other precious metal oxidants, and the catalyst has good application prospects [89].

A three-dimensional spherical $CuBi_2O_4$ nanocolumn array was synthesized by a hydrothermal method for the activation of PMS and PS. The performance of CuB-2.5 for the degradation of 1H-benzotriazole was better than the performance of homogeneous Cu^{2+}, CuO, CuB-microspheres, and a novel $CuBi_2O_4$, consisting of self-assembled spherical nanocolumn arrays (CuB-H). The PMS/an efficient bifunctional catalyst (CuB-2.5) was better than the PS/CuB-2.5 [90]. The catalytic performance of $NiFe_2O_4$ is better than the catalytic performance of Fe_2O_3 (23.5%), Fe_3O_4 (48.0%), NiO (57.6%), and $MnFe_2O_4$ (63.8%). Although the degradation rate of benzoic acid (BA) by $NiFe_2O_4$ is slightly lower than the degradation rate of $CoFe_2O_4$ (86.2%), the leaching rate of nickel (0.265 mol·L^{-1}) is much lower than the leaching rate of cobalt (0.384 mol·L^{-1}) [91]. Graphene can significantly improve the performance of the catalyst. $MnFe_2O_4$-rGO has a lower activation energy (25.7 kJ·mol^{-1}) than $MnFe_2O_4$ (31.7 kJ·mol^{-1}), which shows higher chemical properties, indicating that the introduction of graphene can promote the performance of the catalyst. The $MnFe_2O_4$ and $MnFe_2O_4$-rGO hybrids showed durability in eliminating organic pollutants, excellent Fenton-like activity and an easy separation magnetism [92]. Meanwhile, the oxidation of Fe^{2+} to Fe^{3+} easily causes metal leaching, but the combined use of cerium and iron can inhibit this leaching process [93]. Loading both Fe and Ce on diatomite (DIA) can not only change the catalytic activity of Fe^{2+} but also prevent the agglomeration of metal catalysts, while the removal efficiency of tetracycline on Fe-Ce/DIA under an ultraviolet (UV)-activated persulfate process can reach 86% [94]. The degradation of rhodamine B by Ag@CuO nanocomposite-activated persulfate was better than the degradation of rhodamine by CuO alone [95], whereas the catalytic performance of the MnCeOx composite was better than MnOx, MnOx+CeO_2 and CeO_2 in activated persulfate for the treatment of Acid Orange 7 and Ofloxacin [96]. Activated carbon (AC)-nZVI composites were elsewhere prepared by a hydrothermal method. The ZVI nanoparticles were immobilized on an AC surface to reduce the metal aggregation and Fe ion leaching; therefore, the persulfate/AC-nZVI system provides an alternative method for removing antibiotics from wastewater [97]. Additionally, the copper ferrite/montmorillonite-k10 ($CuFe_2O_4$/MMT-k10) nanocomposite was successfully synthesized by a simple citric acid combustion method. The results showed that $CuFe_2O_4$/MMT-k10 effectively activates PS to remove levofloxacin (LVF) in an aqueous solution [98].

4. Electrochemically Activated Persulfate

The process of electrochemical activation of persulfate has the advantages of strong catalytic ability and mild operating conditions. The electrochemical activation process can obviously enhance the mass transfer and the production of free radicals.

Persulfate anions may be regenerated from the anodic oxidation of sulfate ions [99]:

$$S_2O_8{}^{2-} + e^- \rightarrow SO_4{}^{\bullet -} + SO_4{}^{2-} \quad (18)$$

$$2SO_4{}^{2-} \rightarrow S_2O_8{}^- + 2e^- \quad (19)$$

The disadvantage of iron as a catalyst is that it is difficult to regenerate Fe^{2+} after conversion to Fe^{3+} [100]. In electrochemical oxidation, oxidation degradation is the main reason for removing the chemical oxygen demand (COD) in leachate, and the coagulation of the Fe^{2+}/peroxydisulfate process plays a major role. When the two processes are combined, both oxidation and coagulation play important roles [101].

4.1. Electrochemically Activated Peroxydisulfate

An electrochemically activated persulfate system can effectively remove organic pollutants. In the process of electrochemical activation, hydroxyl radicals, sulfate radicals, and nonradical oxidation are formed to degrade pollutants. The decolorization efficiency of Acid Orange 7 can be improved by the electrochemistry/Fe^{2+}/$S_2O_8^{2-}$ combination, which is positively correlated with the concentration of sulfate and ferrous ions; therefore, reducing the use of superfluous acid by improving the efficiency in other areas is a worthy consideration [102]. Traditional electro-Fenton technology uses two electrodes, which has the problems of a weak electrolysis capacity, a long mass transfer distance, and a low current utilization [103]. The particles were added as the third electrode to solve this problem. Compared with the traditional electro-Fenton system, the specific surface area and oxidation capacity of the three-dimensional electro-Fenton system were increased [104]; therefore, under the optimum conditions, Fe^0 is more suitable than Fe^{2+} when different activators (e.g., Fe^{2+} and Fe^0) and persulfate are added into the three-dimensional electro-Fenton-PS system [105]. Additionally, the results showed that toluene in a surfactant solution can be effectively removed by the electric/Fe^{2+}/persulfate process, and that Fe^{3+} is reduced at the same time [106].

When there are donor electron groups on aromatic molecules, the $SO_4^{\bullet-}$ reaction speed increases [107]. $SO_4^{\bullet-}$ tends to be selective by electron transfer [108]. $SO_4^{\bullet-}$ may oxidize toluene faster than straight-chain aliphatic surfactants [10]. Moreover, sulfate radicals are an effective active substance for the selective degradation of toluene in surfactant washing wastewater [106]. The degradation of sulfamethazine by the electric/Fe^{3+}/PDS process is combined with the activated sludge process. The byproducts produced by the electrochemical treatment are biodegradable, and the combination with biodegradation technology greatly enhances the treatment performance [109]. Ferric ions cannot be regenerated after the activation of persulfate, thus requiring a higher concentration of ferrous ions, which results in a large amount of iron sludge in a system. In addition, excess ferrous ion and sulfate-free radical reactions affect the treatment effect. The "electric/Fe^{3+}/peroxydisulfate" method was used to degrade pollutants, and the degradation of bisphenol A by this process was studied. The Fe^{2+}-activated PDS process was enhanced electrochemically, and the TOC removal efficiency reached 94.3% after 120 min of reaction [110,111]. Natural magnetite can effectively activate PDS to remove AO7 over a wide pH range (3.0–9.0). Moreover, as a green energy conversion technology, microbial fuel cells (MFCs) can achieve a sustainable use of electric energy; thus, AO7 was removed through the establishment of a self-driven electric/natural magnetite/PDS (MFC/NM/PDS) system. The advantages of this process are the abundance of natural magnetite and the power produced by green MFC technology [112].

The electro-assisted heterogeneous bimetallic or multi-metallic catalyst activation process of PDS is also very worthy of study. The degradation of cyclobutyl acid by an electrically assisted heterogeneous persulfate (electricity/Fe-Cu catalyst/$S_2O_8^{2-}$) process was studied. Compared with a single metal catalyst, an Fe-Cu bimetallic catalyst has higher catalytic activity, and its removal efficiency can be close to 100% under favorable conditions [113]. The catalyst ($Mn_{0.6}Zn_{0.4}Fe_2O_4$) for the activation of persulfate to degrade BPA was prepared by the gel method with a waste alkaline Zn-Mn battery as the material. The process also allows the alkaline zinc-manganese battery to be reused. The electro-enhanced activation of PDS using $Mn_{0.6}Zn_{0.4}Fe_2O_4$ made of alkaline Zn-Mn batteries could efficiently degrade BPA. As a result, the redox pairs of Mn^{3+}/Mn^{2+} and Fe^{3+}/Fe^{2+}

were involved in the $Mn_{0.6}Zn_{0.4}Fe_2O_4$ activation of PDS. Zn^{2+} did not participate in the activation of PDS [114].

Iron oxides and other minerals are also used as PDS activators coupled with electrochemical methods to degrade pollutants. The EC/Fe_3O_4/PDS process can completely decolorize AO7, and the Fe_3O_4 particles are stable and can be reused, which reduces the cost; however, when too much catalyst is added, the Fe^{2+} on the particle surface reacts with the sulfate radical, which leads to a decrease in the treatment effect [115]. The electrochemical process was combined with the α-FeOOH activation PDS process, and the EC/α-FeOOH/PDS process was studied. The catalyst (α-FeOOH) maintained its high activity and good stability [116].

Mesoporous silica SBA-15 is an ordered mesoporous molecular sieve that has the advantages of good stability, large pore diameter and large specific surface area [117,118]. Furthermore, the results show that the SBA-15 supported metal catalyst has a high stability and can effectively inhibit metal leaching [119]. The coupling of PS with heterogeneous catalysis (Fe/SBA-15) under the EC technique was a highly effective technique for the degradation of an organic dye in an aqueous solution. Additionally, the EC/Fe/SBA-15/PS process has a higher performance-to-price ratio, compared with other advanced oxidation processes (AOPs) [120]. Iron and cobalt are loaded on SBA-15 to prevent metal leaching and to improve total organic carbon (TOC) removal [121]. Using Fe-Co/SBA-15 as a catalyst, the combination of the electrochemical method and the heterogeneous activation of PDS was an excellent method for the degradation of Orange II (Figure 4) [122].

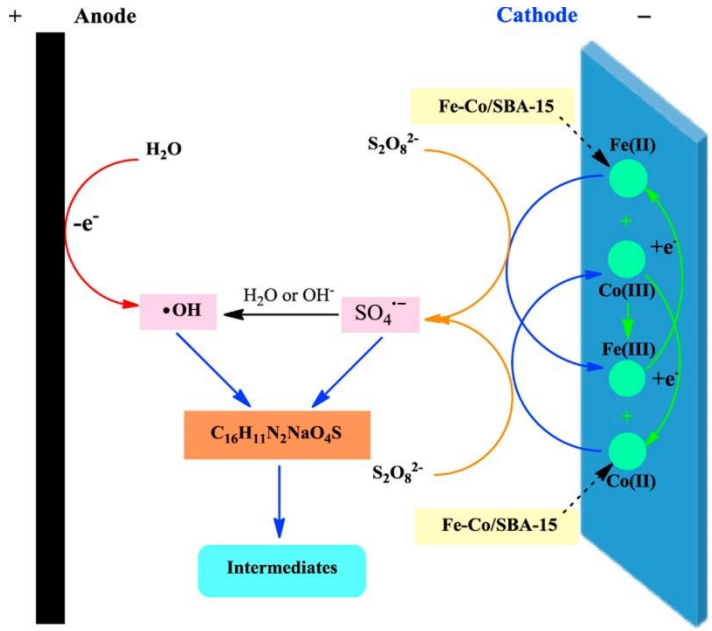

Figure 4. The mechanism of EC/Fe-Co/SBA-15/PDS system. Reprinted with permission from ref. [122]. Copyright 2014 Elsevier B.V.

4.2. Electrochemically Activated Peroxymonosulfate

The asymmetry of PMS makes it more easily activated and produces more sulfate radicals than PDS. Iron-based, copper-based, and cobalt-based catalysts coupled with electrochemical processes to activate PMS have been widely studied. For example, cyclofibrinic acid in water could be effectively removed in the EC/Fe^{3+}/PMS process [123]. Compared with the electro-Fenton system, the electroactive PMS had a higher COD removal. In the electrochemical reactor driven by an uncoated single-chamber microbial fuel cell (MFC/hydronium jarosite (HJ)/PMS), the heterogeneous electro-assisted Fenton system HJ activated PMS was used to decolorize AO7 and the electro-assisted Fenton-like (EAFL) system had a great performance. Its advantage was that it could be driven by the low

voltage generated in uncoated single-room MFCs [124]. By using a Co_3O_4 anode and CuO cathode, the degradation of 4-nitrophenol (4-NP) and the electrocatalytic reduction of CO_2 were combined to convert organic pollutants into liquid fuel in one pot. Electrocatalysis was coupled with AOPs based on $SO_4^{\bullet -}$ to study the degradation of 4-NP on a novel three-dimensional hexagonal array Co_3O_4 anode [125].

Meanwhile, metal-free carbonaceous materials are receiving increasing attention as persulfate-activated heterogeneous catalysts. The electrochemical process combined with the granular activated carbon catalyzed peroxymonosulfate (electro/GAC/PMS) process is better than the traditional electro-oxidation process and GAC/PMS process for the decolorization of AO7 in an aqueous solution. Fourier transform infrared (FTIR) spectroscopy was used to study the fresh GAC samples and the GAC samples used in the GAC/PMS and electro/GAC/PMS processes. The results showed that during the reaction, the number of oxygen-containing groups of GAC in both processes increased, enhancing the activity of PMS to produce sulfate radicals, which was beneficial to the degradation of pollutants [126]. Electrochemically activated persulfate promoted the formation of $^{\bullet}HO$ through water hydrolysis and dissociation on the BDD anode, inhibiting the side reaction of the oxygen evolution and producing a higher concentration of $^{\bullet}HO$ ($>10^{-11}$ mol·L^{-1}) than the electrochemical process based on the BDD anode alone. The electrochemical activation of persulfate on the BDD anode was due mainly to the surface adsorption of $^{\bullet}HO$ rather than non-radical oxidation [127]. Meanwhile, PMS and PDS were activated using graphite and multiwalled carbon nanotubes to degrade sulfamic maloxazole. The results showed that under the same conditions, sulfate radicals play a more important role in the PMS electrochemical activation degradation of pollutants, while non-radical oxidation plays a more important role in the PDS electrochemical activation degradation of pollutants (Figure 5). The application of PMS is superior to PDS in the presence of various resistances to nonradical oxidation of organic pollutants such as atrazine (ATZ), or a high concentration of background ions and natural organic matter (NOM) [34]. Carbamazepine was degraded by electrochemically activated peroxymonosulfate. The cathode was made of activated carbon. Activated peroxymonosulfate consumed less energy than activated peroxydisulfate and in electrolysis coupled with a carbon fiber and peroxymonosulfate system, ROS oxidation (including $^{\bullet}OH$, $SO_4^{\bullet -}$ and $^1O_2$) played an important role in carbamazepine (CBZ) degradation, and $^1O_2$ was produced mainly on the cathode [128].

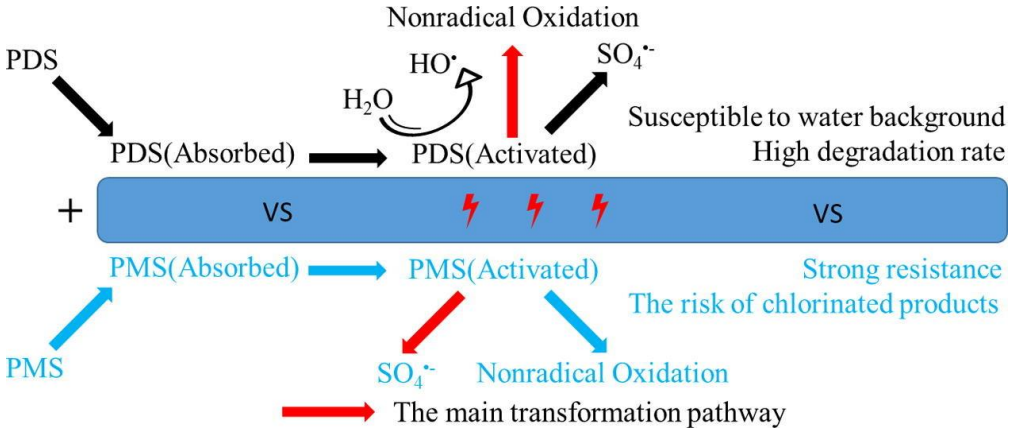

Figure 5. Electrochemically activated PMS and PDS generate active substances for degrading pollutants. Reprinted with permission from ref. [34]. Copyright 2020 Elsevier B.V.

Because the sulfate anions and cathodes were negatively charged, the adsorption of sulfate anions on the electrode surface was reduced, thus, affecting the activation effect. The contact between the persulfate anion and cathode was enhanced by reducing the diffusion distance; therefore, the flow-through cathode (FTC) was developed. In the FTC, the PMS anion is confined in the microchannel, which shortens the diffusion distance, enhances the

contact with the cathode, and increases the output of active substances (Figure 6). The FTC has good performance in the removal of phenol, BPA, and 4-chlorophenol [129].

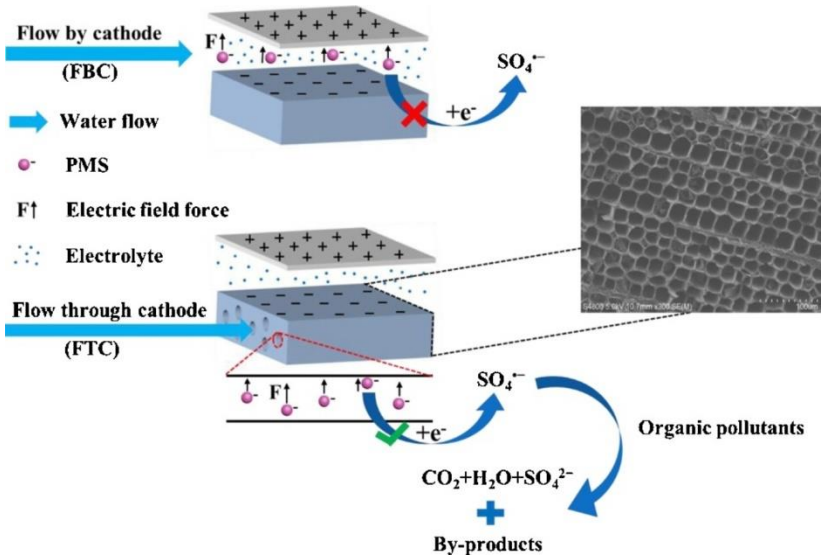

Figure 6. In flow-through cathode (FTC), the mechanism of the decomposition of peroxymonosulfate (PMS) and yield of radicals. Reprinted with permission from ref. [129]. Copyright 2020 Elsevier B.V.

A two-chamber reactor was used to degrade dichloromethane by electrolysis combined with persulfate activation. In this process, the synergistic effect in the anode chamber played a good role. For different electrodes, the effect of the Ti electrode was better than the effect of the TiO_2 electrode and RuO_2/Ti electrode [130]. The decolorization performance of the BDD electro-activated persulfate (BDD-EAP) system for malachite green (MG) was 3.37 times the decolorization performance of the BDD electrochemical oxidation (BDD-EO) system, and the removal capacity of the BDD-EAP system for the TOC was 2.2 times the removal capacity of the BDD-EO system. The BDD-EAP technology decomposed organic compounds without diffusion limitations and avoided pH regulation, which made the EO treatment of organic wastewater more effective and economical [131].

5. Conclusions

In summary, the metal catalysts-activated persulfate and electrochemically-activated persulfate processes for the removal of pollutants have been reviewed. The metal catalysts have wide application prospects in the treatment of pollutants in water. The combination of mixed metal catalysts and electrochemical processes solves the problem of metal leaching to some extent. Good progress has been made in the study of the different metal catalysts in controlling the cost and improving the degradation effect. In the electrochemical advanced oxidation process, the introduction of electricity improves the treatment effect and has been further studied. In the treatment of pollutants in water, hydroxyl radicals and sulfate radicals are the main active substances. On the premise of considering the cost and environmental protection, the leaching rate of metal ions is reduced, and the removal efficiency of pollutants is improved.

Some research findings have been obtained in terms of metal-based heterogeneous catalysts-activated persulfate and electrochemically-activated persulfate processes; however, many challenges still exist. The following aspects are suggested to be considered in future research.

(1) The strategy to detect radicals, namely, the use of chemical probes or spin trapping agents coupled with analytical tools, and practical issues, such as residual PMS, need to be considered before application in a larger-scale study.

(2) It is suggested that future studies study novel reactor designs for heterogeneous catalytic systems based on batch or continuous flow reactor configurations with catalyst recovery to provide a suitable platform to fully exploit the advantages of PMS oxidation processes.

(3) The combination metal-based heterogeneous catalysts-activated persulfate or electrochemically-activated persulfate with other technologies that may prevent catalyst aggregation and electrode passivation, such as membrane technology systems, should be promising in future applications.

(4) It would also be an interesting study to utilize both a cathode and anode in electrochemically-activated persulfate systems, which would help to improve the current utilization efficiency.

Author Contributions: Investigation, conceptualization, and categorization by J.L., Y.L., P.J., B.Z., Z.Z. and Z.T.; writing and editing by J.L. and Y.L.; funding acquisition, editing, and supervision by J.L., X.H., L.W. and X.C. This manuscript was written through contributions of all authors. All authors have read and agreed to the published version of the manuscript.

Funding: This work was kindly supported by the China Postdoctoral Science Foundation (2020T130470, 2018M641656), Scientific Research Plan Project of Tianjin Municipal Education Commission (2017KJ077), National Natural Science Foundation of China (51508385), Tianjin Municipal Education Commission Research Plan Projects (TJPU2k20170112), TGU Grant for Fiber Studies (TGF-21-B3), and The National Youth Talent Support Program.

Data Availability Statement: The datasets used and analyzed during the current study are available from the corresponding references listed.

Conflicts of Interest: The authors declare no conflict of interest.

References

1. Li, J.J.; Wang, H.; Qi, Z.Y.; Ma, C.; Zhang, Z.H.; Zhao, B.; Wang, L.; Zhang, H.W.; Chong, Y.T.; Chen, X.; et al. Kinetics and mechanisms of electrocatalytic hydrodechlorination of diclofenac on Pd-Ni/PPy-rGO/Ni electrodes. *Appl. Catal. B* **2020**, *268*, 118696. [CrossRef]
2. Arthur, R.B.; Ahern, J.C.; Patterson, H.H. Application of BiOX photocatalysts in remediation of persistent organic pollutants. *Catalysts* **2018**, *8*, 604. [CrossRef]
3. Han, S.; Xiao, P.F. Catalytic degradation of tetracycline using peroxymonosulfate activated by cobalt and iron Co-loaded pomelo peel biochar nanocomposite: Characterization, performance and reaction mechanism. *Sep. Purif. Technol.* **2022**, *287*, 120533. [CrossRef]
4. Yang, X.Y.; Cheng, X.W.; Elzatahry, A.A.; Chen, J.Y.; Alghamdi, A.; Deng, Y.H. Recyclable Fenton-like catalyst based on zeolite Y supported ultrafine, highly-dispersed Fe_2O_3 nanoparticles for removal of organics under mild conditions. *Chin. Chem. Lett.* **2019**, *30*, 324–330. [CrossRef]
5. Chen, K.; Wang, G.H.; Li, W.B.; Wan, D.; Hu, Q.; Lu, L.L. Application of response surface methodology for optimization of Orange II removal by heterogeneous Fenton-like process using Fe_3O_4 nanoparticles. *Chin. Chem. Lett.* **2014**, *25*, 1455–1460. [CrossRef]
6. Ji, Q.Q.; Li, J.; Xiong, Z.K.; Lai, B. Enhanced reactivity of microscale Fe/Cu bimetallic particles (mFe/Cu) with persulfate (PS) for *p*-nitrophenol (PNP) removal in aqueous solution. *Chemosphere* **2017**, *172*, 10–20. [CrossRef] [PubMed]
7. Sharma, J.; Mishra, I.M.; Dionysiou, D.D.; Kumar, V. Oxidative removal of Bisphenol A by UV-C/peroxymonosulfate (PMS): Kinetics, influence of co-existing chemicals and degradation pathway. *Chem. Eng. J.* **2015**, *276*, 193–204. [CrossRef]
8. Nfodzo, P.; Choi, H. Sulfate radicals destroy pharmaceuticals and personal care products. *Environ. Eng. Sci.* **2011**, *28*, 605–609. [CrossRef]
9. Zhang, R.C.; Sun, P.Z.; Boyer, T.H.; Zhao, L.; Huang, C.H. Degradation of pharmaceuticals and metabolite in synthetic human urine by UV, UV/H_2O_2, and UV/PDS. *Environ. Sci. Technol.* **2015**, *49*, 3056–3066. [CrossRef]
10. Antoniou, M.G.; de la Cruz, A.A.; Dionysiou, D.D. Intermediates and reaction pathways from the degradation of microcystin-LR with sulfate radicals. *Environ. Sci. Technol.* **2010**, *44*, 7238–7244. [CrossRef]
11. Antoniou, M.G.; de la Cruz, A.A.; Dionysiou, D.D. Degradation of microcystin-LR using sulfate radicals generated through photolysis, thermolysis and e(-) transfer mechanisms. *Appl. Catal. B* **2010**, *96*, 290–298. [CrossRef]
12. Lee, Y.C.; Lo, S.L.; Kuo, J.; Huang, C.P. Promoted degradation of perfluorooctanic acid by persulfate when adding activated carbon. *J. Hazard. Mater.* **2013**, *261*, 463–469. [CrossRef] [PubMed]
13. Ji, Y.F.; Dong, C.X.; Kong, D.Y.; Lu, J.H.; Zhou, Q.S. Heat-activated persulfate oxidation of atrazine: Implications for remediation of groundwater contaminated by herbicides. *Chem. Eng. J.* **2015**, *263*, 45–54. [CrossRef]
14. Guan, Y.H.; Ma, J.; Li, X.C.; Fang, J.Y.; Chen, L.W. Influence of pH on the formation of sulfate and hydroxyl radicals in the UV/peroxymonosulfate system. *Environ. Sci. Technol.* **2011**, *45*, 9308–9314. [CrossRef]

15. Li, N.; Wang, Y.S.; Cheng, X.S.; Dai, H.X.; Yan, B.B.; Chen, G.Y.; Hou, L.A.; Wang, S.B. Influences and mechanisms of phosphate ions onto persulfate activation and organic degradation in water treatment: A review. *Water Res.* **2022**, *222*, 118896. [CrossRef]
16. Cai, C.; Zhang, H.; Zhong, X.; Hou, L.W. Ultrasound enhanced heterogeneous activation of peroxymonosulfate by a bimetallic Fe-Co/SBA-15 catalyst for the degradation of Orange II in water. *J. Hazard. Mater.* **2015**, *283*, 70–79. [CrossRef]
17. Oyekunle, D.T.; Gendy, E.A.; Ifthikar, J.; Chen, Z.Q. Heterogeneous activation of persulfate by metal and non-metal catalyst for the degradation of sulfamethoxazole: A review. *Chem. Eng. J.* **2022**, *437*, 135277. [CrossRef]
18. Guo, R.N.; Zhu, Y.L.; Cheng, X.W.; Li, J.J.; Crittenden, J.C. Efficient degradation of lomefloxacin by Co-Cu-LDH activating peroxymonosulfate process: Optimization, dynamics, degradation pathway and mechanism. *J. Hazard. Mater.* **2020**, *399*, 122966. [CrossRef]
19. Guo, R.N.; Wang, Y.Y.; Li, J.J.; Cheng, X.W.; Dionysiou, D.D. Sulfamethoxazole degradation by visible light assisted peroxymonosulfate process based on nanohybrid manganese dioxide incorporating ferric oxide. *Appl. Catal. B* **2020**, *278*, 119297. [CrossRef]
20. Xu, C.Y.; Yang, G.R.; Li, J.; Zhang, S.Q.; Fang, Y.P.; Peng, F.; Zhang, S.S.; Qiu, R.L. Efficient purification of tetracycline wastewater by activated persulfate with heterogeneous Co-V bimetallic oxides. *J. Colloid Interface Sci.* **2022**, *619*, 188–197. [CrossRef]
21. Zheng, X.X.; Niu, X.J.; Zhang, D.Q.; Lv, M.Y.; Ye, X.Y.; Ma, J.L.; Lin, Z.; Fu, M.L. Metal-based catalysts for persulfate and peroxymonosulfate activation in heterogeneous ways: A review. *Chem. Eng. J.* **2022**, *429*, 132323. [CrossRef]
22. Li, J.J.; Guo, R.N.; Ma, Q.L.; Nengzi, L.C.; Cheng, X.W. Efficient removal of organic contaminant via activation of potassium persulfate by γ-Fe_2O_3/α-MnO_2 nanocomposite. *Sep. Purif. Technol.* **2019**, *227*, 115669. [CrossRef]
23. Qin, Y.H.; Sun, M.; Liu, H.J.; Qu, J.H. AuPd/Fe_3O_4-based three-dimensional electrochemical system for efficiently catalytic degradation of 1-butyl-3-methylimidazolium hexafluorophosphate. *Electrochim. Acta* **2015**, *186*, 328–336. [CrossRef]
24. Sun, X.P.; Liu, Z.B.; Sun, Z.R. Electro-enhanced degradation of atrazine via Co-Fe oxide modified graphite felt composite cathode for persulfate activation. *Chem. Eng. J.* **2022**, *433*, 133789. [CrossRef]
25. Matzek, L.W.; Tipton, M.J.; Farmer, A.T.; Steen, A.D.; Carter, K.E. Understanding electrochemically activated persulfate and its application to ciprofloxacin abatement. *Environ. Sci. Technol.* **2018**, *52*, 5875–5883. [CrossRef]
26. Cai, J.J.; Zhou, M.H.; Zhang, Q.Z.; Tian, Y.S.; Song, G. The radical and non-radical oxidation mechanism of electrochemically activated persulfate process on different cathodes in divided and undivided cell. *J. Hazard. Mater.* **2021**, *416*, 125804. [CrossRef]
27. Liang, C.J.; Bruell, C.J.; Marley, M.C.; Sperry, K.L. Thermally activated persulfate oxidation of trichloroethylene (TCE) and 1,1,1-trichloroethane (TCA) in aqueous systems and soil slurries. *Soil Sediment Contam.* **2003**, *12*, 207–228. [CrossRef]
28. Gogate, P.R.; Pandit, A.B. A review of imperative technologies for wastewater treatment I: Oxidation technologies at ambient conditions. *Adv. Environ. Res.* **2004**, *8*, 501–551. [CrossRef]
29. Anipsitakis, G.P.; Dionysiou, D.D. Degradation of organic contaminants in water with sulfate radicals generated by the conjunction of peroxymonosulfate with cobalt. *Environ. Sci. Technol.* **2003**, *37*, 4790–4797. [CrossRef]
30. Bandala, E.R.; Pelaez, M.A.; Dionysiou, D.D.; Gelover, S.; Garcia, J.; Macias, D. Degradation of 2,4-dichlorophenoxyacetic acid (2,4-D) using cobalt-peroxymonosulfate in Fenton-like process. *J. Photoch. Photobio. A* **2007**, *186*, 357–363. [CrossRef]
31. Tsitonaki, A.; Petri, B.; Crimi, M.; Mosbaek, H.; Siegrist, R.L.; Bjerg, P.L. In situ chemical oxidation of contaminated soil and groundwater using persulfate: A review. *Crit. Rev. Environ. Sci. Technol.* **2010**, *40*, 55–91. [CrossRef]
32. Yang, S.Y.; Wang, P.; Yang, X.; Shan, L.; Zhang, W.Y.; Shao, X.T.; Niu, R. Degradation efficiencies of azo dye Acid Orange 7 by the interaction of heat, UV and anions with common oxidants: Persulfate, peroxymonosulfate and hydrogen peroxide. *J. Hazard. Mater.* **2010**, *179*, 552–558. [CrossRef] [PubMed]
33. Waldemer, R.H.; Tratnyek, P.G.; Johnson, R.L.; Nurmi, J.T. Oxidation of chlorinated ethenes by heat-activated persulfate: Kinetics and products. *Environ. Sci. Technol.* **2007**, *41*, 1010–1015. [CrossRef] [PubMed]
34. Song, H.R.; Yan, L.X.; Wang, Y.W.; Jiang, J.; Ma, J.; Li, C.P.; Wang, G.; Gu, J.; Liu, P. Electrochemically activated PMS and PDS: Radical oxidation versus nonradical oxidation. *Chem. Eng. J.* **2020**, *391*, 123560. [CrossRef]
35. Liang, C.J.; Bruell, C.J.; Marley, M.C.; Sperry, K.L. Persulfate oxidation for in situ remediation of TCE. I. Activated by ferrous ion with and without a persulfate-thiosulfate redox couple. *Chemosphere* **2004**, *55*, 1213–1223. [CrossRef]
36. Yuan, S.H.; Liao, P.; Alshawabkeh, A.N. Electrolytic manipulation of persulfate reactivity by iron electrodes for trichloroethylene degradation in groundwater. *Environ. Sci. Technol.* **2014**, *48*, 656–663. [CrossRef]
37. Wang, S.L.; Zhou, N. Removal of carbamazepine from aqueous solution using sono-activated persulfate process. *Ultrason. Sonochem.* **2016**, *29*, 156–162. [CrossRef]
38. He, L.Y.; Chen, H.; Wu, L.; Zhang, Z.L.; Ma, Y.F.; Zhu, J.; Liu, J.X.; Yan, X.K.; Li, H.; Yang, L. Synergistic heat/UV activated persulfate for the treatment of nanofiltration concentrated leachate. *Ecotoxicol. Environ. Saf.* **2021**, *208*, 111522. [CrossRef]
39. Fang, G.D.; Gao, J.; Dionysiou, D.D.; Liu, C.; Zhou, D.M. Activation of persulfate by quinones: Free radical reactions and implication for the degradation of PCBs. *Environ. Sci. Technol.* **2013**, *47*, 4605–4611. [CrossRef]
40. Wang, S.L.; Ning, Z.; Si, W.; Qi, Z.; Zhi, Y. Modeling the oxidation kinetics of sono-activated persulfate's process on the degradation of humic acid. *Ultrason. Sonochem.* **2015**, *23*, 128–134. [CrossRef]
41. Bennedsen, L.R.; Muff, J.; Sogaard, E.G. Influence of chloride and carbonates on the reactivity of activated persulfate. *Chemosphere* **2012**, *86*, 1092–1097. [CrossRef] [PubMed]
42. Hu, P.D.; Long, M.C. Cobalt-catalyzed sulfate radical-based advanced oxidation: A review on heterogeneous catalysts and applications. *Appl. Catal. B* **2016**, *181*, 103–117. [CrossRef]

43. Anipsitakis, G.P.; Stathatos, E.; Dionysiou, D.D. Heterogeneous activation of oxone using Co_3O_4. *J. Phys. Chem. B* **2005**, *109*, 13052–13055. [CrossRef] [PubMed]
44. Sun, H.Q.; Liang, H.W.; Zhou, G.L.; Wang, S.B. Supported cobalt catalysts by one-pot aqueous combustion synthesis for catalytic phenol degradation. *J. Colloid Interface Sci.* **2013**, *394*, 394–400. [CrossRef]
45. Ji, F.; Li, C.; Liu, Y.; Liu, P. Heterogeneous activation of peroxymonosulfate by Cu/ZSM5 for decolorization of Rhodamine B. *Sep. Purif. Technol.* **2014**, *135*, 1–6. [CrossRef]
46. Ji, F.; Li, C.L.; Deng, L. Performance of CuO/Oxone system: Heterogeneous catalytic oxidation of phenol at ambient conditions. *Chem. Eng. J.* **2011**, *178*, 239–243. [CrossRef]
47. Fu, C.; Yi, X.L.; Liu, Y.; Zhou, H. Cu^{2+} activated persulfate for sulfamethazine degradation. *Chemosphere* **2020**, *257*, 127294. [CrossRef]
48. Ye, Y.X.; Wan, J.; Li, Q.; Huang, Y.B.; Pan, F.; Xia, D.S. Catalytic oxidation of dyeing wastewater by copper oxide activating persulfate: Performance, mechanism and application. *Int. J. Environ. Res.* **2021**, *15*, 1–10. [CrossRef]
49. Zhao, J.Y.; Zhang, Y.B.; Quan, X.; Chen, S. Enhanced oxidation of 4-chlorophenol using sulfate radicals generated from zero-valent iron and peroxydisulfate at ambient temperature. *Sep. Purif. Technol.* **2010**, *71*, 302–307. [CrossRef]
50. Liang, C.J.; Guo, Y.Y. Mass transfer and chemical oxidation of naphthalene particles with zerovalent iron activated persulfate. *Environ. Sci. Technol.* **2010**, *44*, 8203–8208. [CrossRef]
51. Liang, C.J.; Lai, M.C. Trichloroethylene degradation by zero valent iron activated persulfate oxidation. *Environ. Eng. Sci.* **2008**, *25*, 1071–1077. [CrossRef]
52. Oh, S.Y.; Kim, H.W.; Park, J.M.; Park, H.S.; Yoon, C. Oxidation of polyvinyl alcohol by persulfate activated with heat, Fe^{2+}, and zero-valent iron. *J. Hazard. Mater.* **2009**, *168*, 346–351. [CrossRef]
53. Oh, S.Y.; Kang, S.G.; Chiu, P.C. Degradation of 2,4-dinitrotoluene by persulfate activated with zero-valent iron. *Sci. Total Environ.* **2010**, *408*, 3464–3468. [CrossRef] [PubMed]
54. Volpe, A.; Pagano, M.; Mascolo, G.; Lopez, A.; Ciannarella, R.; Locaputo, V. Simultaneous Cr(VI) reduction and non-ionic surfactant oxidation by peroxymonosulphate and iron powder. *Chemosphere* **2013**, *91*, 1250–1256. [CrossRef] [PubMed]
55. Hussain, I.; Zhang, Y.Q.; Huang, S.B.; Du, X.Z. Degradation of *p*-chloroaniline by persulfate activated with zero-valent iron. *Chem. Eng. J.* **2012**, *203*, 269–276. [CrossRef]
56. Rastogi, A.; Ai-Abed, S.R.; Dionysiou, D.D. Sulfate radical-based ferrous-peroxymonosulfate oxidative system for PCBs degradation in aqueous and sediment systems. *Appl. Catal. B* **2009**, *85*, 171–179. [CrossRef]
57. Ji, F.; Li, C.L.; Wei, X.Y.; Yu, J. Efficient performance of porous Fe_2O_3 in heterogeneous activation of peroxymonosulfate for decolorization of Rhodamine B. *Chem. Eng. J.* **2013**, *231*, 434–440. [CrossRef]
58. Oh, W.D.; Lua, S.K.; Dong, Z.L.; Lim, T.T. High surface area DPA-hematite for efficient detoxification of bisphenol A via peroxymonosulfate activation. *J. Mater. Chem. A* **2014**, *2*, 15836–15845. [CrossRef]
59. Gong, F.; Wang, L.; Li, D.W.; Zhou, F.Y.; Yao, Y.Y.; Lu, W.T.; Huang, S.Q.; Chen, W.X. An effective heterogeneous iron-based catalyst to activate peroxymonosulfate for organic contaminants removal. *Chem. Eng. J.* **2015**, *267*, 102–110. [CrossRef]
60. Tan, C.Q.; Gao, N.Y.; Deng, Y.; Deng, J.; Zhou, S.Q.; Li, J.; Xin, X.Y. Radical induced degradation of acetaminophen with Fe_3O_4 magnetic nanoparticles as heterogeneous activator of peroxymonosulfate. *J. Hazard. Mater.* **2014**, *276*, 452–460. [CrossRef]
61. Rao, L.J.; Yang, Y.F.; Liu, X.D.; Huang, Y.F.; Chen, M.X.; Yao, Y.Y.; Wang, W.T. Heterogeneous activation of persulfate by supporting ferric oxalate onto activated carbon fibers for organic contaminants removal. *Mater. Res. Bull.* **2020**, *130*, 110919. [CrossRef]
62. Zhao, J.J.; Sun, Y.J.; Zhang, Y.; Zhang, B.T.; Yin, M.; Chen, L. Heterogeneous activation of persulfate by activated carbon supported iron for efficient amoxicillin degradation. *Environ. Technol. Innov.* **2021**, *21*, 101259. [CrossRef]
63. Shao, F.L.; Wang, Y.J.; Mao, Y.R.; Shao, T.; Shang, J.G. Degradation of tetracycline in water by biochar supported nanosized iron activated persulfate. *Chemosphere* **2020**, *261*, 127844. [CrossRef] [PubMed]
64. Pervez, M.N.; He, W.; Zarra, T.; Naddeo, V.; Zhao, Y.P. New sustainable approach for the production of Fe_3O_4/Graphene oxide-activated persulfate system for dye removal in real wastewater. *Water* **2020**, *12*, 733. [CrossRef]
65. Zhang, W.; Tang, G.; Yan, J.W.; Zhao, L.B.; Zhou, X.; Wang, H.L.; Feng, Y.K.; Guo, Y.F.; Wu, J.F.; Chen, W.T.; et al. The decolorization of methyl orange by persulfate activated with natural vanadium-titanium magnetite. *Appl. Surf. Sci.* **2020**, *509*, 144886. [CrossRef]
66. Zhang, X.; Qin, Y.Z.; Zhang, W.T.; Zhang, Y.L.; Yuan, G.E. Oxidative degradation of Orange G in aqueous solution by persulfate activated with pyrite. *Water Sci. Technol.* **2020**, *82*, 185–193. [CrossRef] [PubMed]
67. Ning, H.; Zhai, Y.B.; Li, S.H.; Liu, X.M.; Wang, T.F.; Wang, B.; Liu, Y.L.; Qiu, Z.Z.; Li, C.T.; Zhu, Y. Fe(II) activated persulfate assisted hydrothermal conversion of sewage sludge: Focusing on nitrogen transformation mechanism and removal effectiveness. *Chemosphere* **2020**, *244*, 125473. [CrossRef] [PubMed]
68. Saputra, E.; Muhammad, S.; Sun, H.Q.; Ang, H.M.; Tade, M.O.; Wang, S.B. Manganese oxides at different oxidation states for heterogeneous activation of peroxymonosulfate for phenol degradation in aqueous solutions. *Appl. Catal. B* **2013**, *142*, 729–735. [CrossRef]
69. Saputra, E.; Muhammad, S.; Sun, H.Q.; Ang, H.M.; Tade, M.O.; Wang, S.B. Shape-controlled activation of peroxymonosulfate by single crystal alpha-Mn_2O_3 for catalytic phenol degradation in aqueous solution. *Appl. Catal. B* **2014**, *154*, 246–251. [CrossRef]
70. Saputra, E.; Muhammad, S.; Sun, H.Q.; Patel, A.; Shukla, P.; Zhu, Z.H.; Wang, S.B. Alpha-MnO_2 activation of peroxymonosulfate for catalytic phenol degradation in aqueous solutions. *Catal. Commun.* **2012**, *26*, 144–148. [CrossRef]

71. Wang, Y.X.; Indrawirawan, S.; Duan, X.G.; Sun, H.Q.; Ang, H.M.; Tade, M.O.; Wang, S.B. New insights into heterogeneous generation and evolution processes of sulfate radicals for phenol degradation over one-dimensional alpha-MnO_2 nanostructures. *Chem. Eng. J.* **2015**, *266*, 12–20. [CrossRef]
72. Wang, Y.X.; Sun, H.Q.; Ang, H.M.; Tade, M.O.; Wang, S.B. Synthesis of magnetic core/shell carbon nanosphere supported manganese catalysts for oxidation of organics in water by peroxymonosulfate. *J. Colloid Interface Sci.* **2014**, *433*, 68–75. [CrossRef] [PubMed]
73. Wang, Y.X.; Sun, H.Q.; Ang, H.M.; Tade, M.O.; Wang, S.B. Facile synthesis of hierarchically structured magnetic MnO_2/$ZnFe_2O_4$ hybrid materials and their performance in heterogeneous activation of peroxymonosulfate. *ACS Appl. Mater. Interfaces* **2014**, *6*, 19914–19923. [CrossRef] [PubMed]
74. Tang, D.D.; Zhang, G.K.; Guo, S. Efficient activation of peroxymonosulfate by manganese oxide for the degradation of azo dye at ambient condition. *J. Colloid Interface Sci.* **2015**, *454*, 44–51. [CrossRef] [PubMed]
75. Liang, H.W.; Sun, H.Q.; Patel, A.; Shukla, P.; Zhu, Z.H.; Wang, S.B. Excellent performance of mesoporous Co_3O_4/MnO_2 nanoparticles in heterogeneous activation of peroxymonosulfate for phenol degradation in aqueous solutions. *Appl. Catal. B* **2012**, *127*, 330–335. [CrossRef]
76. Liu, J.; Zhao, Z.W.; Shao, P.H.; Cui, F.Y. Activation of peroxymonosulfate with magnetic Fe_3O_4-MnO_2 core-shell nanocomposites for 4-chlorophenol degradation. *Chem. Eng. J.* **2015**, *262*, 854–861. [CrossRef]
77. Luo, S.L.; Duan, L.; Sun, B.Z.; Wei, M.Y.; Li, X.X.; Xu, A.H. Manganese oxide octahedral molecular sieve (OMS-2) as an effective catalyst for degradation of organic dyes in aqueous solutions in the presence of peroxymonosulfate. *Appl. Catal. B* **2015**, *164*, 92–99. [CrossRef]
78. Ren, Y.M.; Lin, L.Q.; Ma, J.; Yang, J.; Feng, J.; Fan, Z.J. Sulfate radicals induced from peroxymonosulfate by magnetic ferrospinel MFe_2O_4 (M = Co, Cu, Mn, and Zn) as heterogeneous catalysts in the water. *Appl. Catal. B* **2015**, *165*, 572–578. [CrossRef]
79. Stoyanova, M.; Slavova, I.; Christoskova, S.; Ivanova, V. Catalytic performance of supported nanosized cobalt and iron-cobalt mixed oxides on MgO in oxidative degradation of Acid Orange 7 azo dye with peroxymonosulfate. *Appl. Catal. A* **2014**, *476*, 121–132. [CrossRef]
80. You, Y.; Shi, Z.K.; Li, Y.H.; Zhao, Z.J.; He, B.; Cheng, X.W. Magnetic cobalt ferrite biochar composite as peroxymonosulfate activator for removal of lomefloxacin hydrochloride. *Sep. Purif. Technol.* **2021**, *272*, 118889. [CrossRef]
81. Hu, L.X.; Yang, F.; Zou, L.P.; Yuan, H.; Hu, X. Fe/SBA-15 catalyst coupled with peroxymonosulfate for heterogeneous catalytic degradation of rhodamine B in water. *Chin. J. Catal.* **2015**, *36*, 1785–1797. [CrossRef]
82. Xu, L.J.; Chu, W.; Gan, L. Environmental application of graphene-based $CoFe_2O_4$ as an activator of peroxymonosulfate for the degradation of a plasticizer. *Chem. Eng. J.* **2015**, *263*, 435–443. [CrossRef]
83. Yao, Y.J.; Yang, Z.H.; Zhang, D.W.; Peng, W.C.; Sun, H.Q.; Wang, S.B. Magnetic $CoFe_2O_4$-Graphene hybrids: Facile synthesis, characterization, and catalytic properties. *Ind. Eng. Chem. Res.* **2012**, *51*, 6044–6051. [CrossRef]
84. Du, Y.C.; Ma, W.J.; Liu, P.X.; Zou, B.H.; Ma, J. Magnetic $CoFe_2O_4$ nanoparticles supported on titanate nanotubes ($CoFe_2O_4$/TNTs) as a novel heterogeneous catalyst for peroxymonosulfate activation and degradation of organic pollutants. *J. Hazard. Mater.* **2016**, *308*, 58–66. [CrossRef]
85. Yao, Y.J.; Cai, Y.M.; Wu, G.D.; Wei, F.Y.; Li, X.Y.; Chen, H.; Wang, S.B. Sulfate radicals induced from peroxymonosulfate by cobalt manganese oxides ($CoxMn_3$-xO_4) for Fenton-Like reaction in water. *J. Hazard. Mater.* **2015**, *296*, 128–137. [CrossRef]
86. Ding, Y.B.; Zhu, L.H.; Wang, N.; Tang, H.Q. Sulfate radicals induced degradation of tetrabromobisphenol A with nanoscaled magnetic $CuFe_2O_4$ as a heterogeneous catalyst of peroxymonosulfate. *Appl. Catal. B* **2013**, *129*, 153–162. [CrossRef]
87. Oh, W.D.; Lua, S.K.; Dong, Z.L.; Lim, T.T. Performance of magnetic activated carbon composite as peroxymonosulfate activator and regenerable adsorbent via sulfate radical-mediated oxidation processes. *J. Hazard. Mater.* **2015**, *284*, 1–9. [CrossRef]
88. Xu, Y.; Ai, J.; Zhang, H. The mechanism of degradation of bisphenol A using the magnetically separable $CuFe_2O_4$/peroxymonosulfate heterogeneous oxidation process. *J. Hazard. Mater.* **2016**, *309*, 87–96. [CrossRef]
89. Bikkarolla, S.K.; Papakonstantinou, P. $CuCo_2O_4$ nanoparticles on nitrogenated graphene as highly efficient oxygen evolution catalyst. *J. Power Sources* **2015**, *281*, 243–251. [CrossRef]
90. Oh, W.D.; Lua, S.K.; Dong, Z.L.; Lim, T.T. A novel three-dimensional spherical $CuBi_2O_4$ consisting of nanocolumn arrays with persulfate and peroxymonosulfate activation functionalities for 1H-benzotriazole removal. *Nanoscale* **2015**, *7*, 8149–8158. [CrossRef]
91. Wang, Z.L.; Du, Y.C.; Liu, Y.L.; Zou, B.H.; Xiao, J.Y.; Ma, J. Degradation of organic pollutants by $NiFe_2O_4$/peroxymonosulfate: Efficiency, influential factors and catalytic mechanism. *RSC Adv.* **2016**, *6*, 11040–11048. [CrossRef]
92. Yao, Y.J.; Cai, Y.M.; Lu, F.; Wei, F.Y.; Wang, X.Y.; Wang, S.B. Magnetic recoverable $MnFe_2O_4$ and $MnFe_2O_4$-graphene hybrid as heterogeneous catalysts of peroxymonosulfate activation for efficient degradation of aqueous organic pollutants. *J. Hazard. Mater.* **2014**, *270*, 61–70. [CrossRef] [PubMed]
93. Abbasi, M.; Mirzaei, A.A.; Atashi, H. Hydrothermal synthesis of Fe-Ni-Ce nano-structure catalyst for Fischer-Tropsch synthesis: Characterization and catalytic performance. *J. Alloys Compd.* **2019**, *799*, 546–555. [CrossRef]
94. Lv, C.N.; Shi, J.D.; Tang, Q.J.; Hu, Q. Tetracycline removal by activating persulfate with diatomite loading of Fe and Ce. *Molecules* **2020**, *25*, 5531. [CrossRef] [PubMed]
95. Zhang, T.; Zhou, T.T.; He, L.; Xu, D.Q.; Bai, L. Oxidative degradation of Rhodamine B by Ag@CuO nanocomposite activated persulfate. *Synth. Met.* **2020**, *267*, 116479. [CrossRef]
96. Niu, L.J.; Xian, G.; Long, Z.Q.; Zhang, G.M.; Zhu, J.; Li, J.W. MnCeOx with high efficiency and stability for activating persulfate to degrade AO7 and ofloxacin. *Ecotoxicol. Environ. Saf.* **2020**, *191*, 110228. [CrossRef]

97. Zhang, Y.; Zhang, B.T.; Teng, Y.G.; Zhao, J.J. Activated carbon supported nanoscale zero valent iron for cooperative adsorption and persulfate-driven oxidation of ampicillin. *Environ. Technol. Innov.* **2020**, *19*, 100956. [CrossRef]
98. Yang, J.Y.; Huang, M.Y.; Wang, S.S.; Mao, X.Y.; Hu, Y.M.; Chen, X. Efficient removal of levofloxacin by activated persulfate with magnetic $CuFe_2O_4$/MMT-k10 nanocomposite: Characterization, response surface methodology, and degradation mechanism. *Water* **2020**, *12*, 3583. [CrossRef]
99. Chen, W.S.; Jhou, Y.C.; Huang, C.P. Mineralization of dinitrotoluenes in industrial wastewater by electro-activated persulfate oxidation. *Chem. Eng. J.* **2014**, *252*, 166–172. [CrossRef]
100. Wang, Y.R.; Chu, W. Degradation of 2,4,5-trichlorophenoxyacetic acid by a novel Electro-Fe(II)/Oxone process using iron sheet as the sacrificial anode. *Water Res.* **2011**, *45*, 3883–3889. [CrossRef]
101. Zhang, H.; Wang, Z.; Liu, C.C.; Guo, Y.Z.; Shan, N.; Meng, C.X.; Sun, L.Y. Removal of COD from landfill leachate by an electro/Fe^{2+}/peroxydisulfate process. *Chem. Eng. J.* **2014**, *250*, 76–82. [CrossRef]
102. Wu, J.; Zhang, H.; Qiu, J.J. Degradation of Acid Orange 7 in aqueous solution by a novel electro/Fe^{2+}/peroxydisulfate process. *J. Hazard. Mater.* **2012**, *215*, 138–145. [CrossRef] [PubMed]
103. Wang, C.; Huang, Y.K.; Zhao, Q.; Ji, M. Treatment of secondary effluent using a three-dimensional electrode system: COD removal, biotoxicity assessment, and disinfection effects. *Chem. Eng. J.* **2014**, *243*, 1–6.
104. Li, M.; Zhao, F.P.; Sillanpaa, M.; Meng, Y.; Yin, D.L. Electrochemical degradation of 2-diethylamino-6-methyl-4-hydroxypyrimidine using three-dimensional electrodes reactor with ceramic particle electrodes. *Sep. Purif. Technol.* **2015**, *156*, 588–595. [CrossRef]
105. Long, Y.Y.; Feng, Y.; Li, X.; Suo, N.; Chen, H.; Wang, Z.W.; Yu, Y.Z. Removal of diclofenac by three-dimensional electro-Fenton-persulfate (3D electro-Fenton-PS). *Chemosphere* **2019**, *219*, 1024–1031. [CrossRef] [PubMed]
106. Long, A.H.; Zhang, H. Selective oxidative degradation of toluene for the recovery of surfactant by an electro/Fe^{2+}/persulfate process. *Environ. Sci. Pollut. Res.* **2015**, *22*, 11606–11616. [CrossRef] [PubMed]
107. Long, A.H.; Lei, Y.; Zhang, H. In situ chemical oxidation of organic contaminated soil and groundwater using activated persulfate process. *Prog. Chem.* **2014**, *26*, 898–908.
108. Anipsitakis, G.P.; Dionysiou, D.D.; Gonzalez, M.A. Cobalt-mediated activation of peroxymonosulfate and sulfate radical attack on phenolic compounds. Implications of chloride ions. *Environ. Sci. Technol.* **2006**, *40*, 1000–1007. [CrossRef]
109. Ledjeri, A.; Yahiaoui, I.; Kadji, H.; Aissani-Benissad, F.; Amrane, A.; Fourcade, F. Combination of the Electro/Fe^{3+}/peroxydisulfate (PDS) process with activated sludge culture for the degradation of sulfamethazine. *Environ. Toxicol. Phar.* **2017**, *53*, 34–39. [CrossRef]
110. Hu, C.Y.; Hou, Y.Z.; Lin, Y.L.; Deng, Y.G.; Hua, S.J.; Du, Y.F.; Chen, C.W.; Wu, C.H. Investigation of iohexol degradation kinetics by using heat-activated persulfate. *Chem. Eng. J.* **2020**, *379*, 122403. [CrossRef]
111. Lin, H.; Wu, J.; Zhang, H. Degradation of bisphenol A in aqueous solution by a novel electro/Fe^{3+}/peroxydisulfate process. *Sep. Purif. Technol.* **2013**, *117*, 18–23. [CrossRef]
112. Yan, S.D.; Xiong, W.H.; Xing, S.Y.; Shao, Y.Q.; Guo, R.; Zhang, H. Oxidation of organic contaminant in a self-driven electro/natural maghemite/peroxydisulfate system: Efficiency and mechanism. *Sci. Total Environ.* **2017**, *599*, 1181–1190. [CrossRef] [PubMed]
113. Lin, H.; Zhong, X.; Ciotonea, C.; Fan, X.H.; Mao, X.Y.; Li, Y.T.; Deng, B.; Zhang, H.; Royer, S. Efficient degradation of clofibric acid by electro-enhanced peroxydisulfate activation with Fe-Cu/SBA-15 catalyst. *Appl. Catal. B* **2018**, *230*, 1–10. [CrossRef]
114. Deng, B.; Li, Y.T.; Tan, W.H.; Wang, Z.X.; Yu, Z.W.; Xing, S.Y.; Lin, H.; Zhang, H. Degradation of bisphenol A by electro-enhanced heterogeneous activation of peroxydisulfate using Mn-Zn ferrite from spent alkaline Zn-Mn batteries. *Chemosphere* **2018**, *204*, 178–185. [CrossRef] [PubMed]
115. Lin, H.; Zhang, H.; Hou, L.W. Degradation of C. I. Acid Orange 7 in aqueous solution by a novel electro/Fe_3O_4/PDS process. *J. Hazard. Mater.* **2014**, *276*, 182–191. [CrossRef]
116. Lin, H.; Li, Y.T.; Mao, X.Y.; Zhang, H. Electro-enhanced goethite activation of peroxydisulfate for the decolorization of Orange II at neutral pH: Efficiency, stability and mechanism. *J. Taiwan Inst. Chem. Eng.* **2016**, *65*, 390–398. [CrossRef]
117. Huang, R.H.; Yan, H.H.; Li, L.S.; Deng, D.Y.; Shu, Y.H.; Zhang, Q.Y. Catalytic activity of Fe/SBA-15 for ozonation of dimethyl phthalate in aqueous solution. *Appl. Catal. B* **2011**, *106*, 264–271. [CrossRef]
118. Hu, L.X.; Yang, F.; Lu, W.C.; Hao, Y.; Yuan, H. Heterogeneous activation of oxone with CoMg/SBA-15 for the degradation of dye Rhodamine B in aqueous solution. *Appl. Catal. B* **2013**, *134*, 7–18. [CrossRef]
119. Hu, L.X.; Yang, X.P.; Dang, S.T. An easily recyclable Co/SBA-15 catalyst: Heterogeneous activation of peroxymonosulfate for the degradation of phenol in water. *Appl. Catal. B* **2011**, *102*, 19–26. [CrossRef]
120. Cai, C.; Zhang, Z.Y.; Zhang, H. Electro-assisted heterogeneous activation of persulfate by Fe/SBA-15 for the degradation of Orange II. *J. Hazard. Mater.* **2016**, *313*, 209–218. [CrossRef]
121. Melero, J.A.; Calleja, G.; Martinez, F.; Molina, R. Nanocomposite of crystalline Fe_2O_3 and CuO particles and mesostructured SBA-15 silica as an active catalyst for wet peroxide oxidation processes. *Catal. Commun.* **2006**, *7*, 478–483. [CrossRef]
122. Cai, C.; Zhang, H.; Zhong, X.; Hou, L.W. Electrochemical enhanced heterogeneous activation of peroxydisulfate by Fe-Co/SBA-15 catalyst for the degradation of Orange II in water. *Water Res.* **2014**, *66*, 473–485. [CrossRef] [PubMed]
123. Lin, H.; Wu, J.; Zhang, H. Degradation of clofibric acid in aqueous solution by an EC/Fe^{3+}/PMS process. *Chem. Eng. J.* **2014**, *244*, 514–521. [CrossRef]
124. Yan, S.D.; Geng, J.Y.; Guo, R.; Du, Y.; Zhang, H. Hydronium jarosite activation of peroxymonosulfate for the oxidation of organic contaminant in an electrochemical reactor driven by microbial fuel cell. *J. Hazard. Mater.* **2017**, *333*, 358–368. [CrossRef] [PubMed]

125. Zou, J.P.; Chen, X.; Liu, S.S.; Xing, Q.J.; Dong, W.H.; Luo, X.B.; Dai, W.L.; Xiao, X.; Luo, J.M.; Crittenden, J. Electrochemical oxidation and advanced oxidation processes using a 3D hexagonal Co_3O_4 array anode for 4-nitrophenol decomposition coupled with simultaneous CO_2 conversion to liquid fuels via a flower-like CuO cathode. *Water Res.* **2019**, *150*, 330–339. [CrossRef]
126. Li, J.; Lin, H.; Zhu, K.M.; Zhang, H. Degradation of Acid Orange 7 using peroxymonosulfate catalyzed by granulated activated carbon and enhanced by electrolysis. *Chemosphere* **2017**, *188*, 139–147. [CrossRef]
127. Song, H.R.; Yan, L.X.; Jiang, J.; Ma, J.; Zhang, Z.X.; Zhang, J.M.; Liu, P.X.; Yang, T. Electrochemical activation of persulfates at BDD anode: Radical or nonradical oxidation? *Water Res.* **2018**, *128*, 393–401. [CrossRef]
128. Liu, Z.; Ding, H.J.; Zhao, C.; Wang, T.; Wang, P.; Dionysiou, D.D. Electrochemical activation of peroxymonosulfate with ACF cathode: Kinetics, influencing factors, mechanism, and application potential. *Water Res.* **2019**, *159*, 111–121. [CrossRef]
129. Zhang, Y.; Kang, W.D.; Yu, H.T.; Chen, S.; Quan, X. Electrochemical activation of peroxymonosulfate in cathodic micro-channels for effective degradation of organic pollutants in wastewater. *J. Hazard. Mater.* **2020**, *398*, 122879. [CrossRef]
130. Lei, J.M.; Cai, Q.; Yang, Q.; Wang, Y.Y. Oxidative removal of dichloromethane by electro-activated persulfate in a dual-chamber reactor. *Environ. Eng. Sci.* **2020**, *37*, 596–605. [CrossRef]
131. Miao, D.T.; Liu, G.S.; Wei, Q.P.; Hu, N.X.; Zheng, K.Z.; Zhu, C.W.; Liu, T.; Zhou, K.C.; Yu, Z.M.; Ma, L. Electro-activated persulfate oxidation of malachite green by boron-doped diamond (BDD) anode: Effect of degradation process parameters. *Water Sci. Technol.* **2020**, *81*, 925–935. [CrossRef] [PubMed]